Supplementary Figure S1

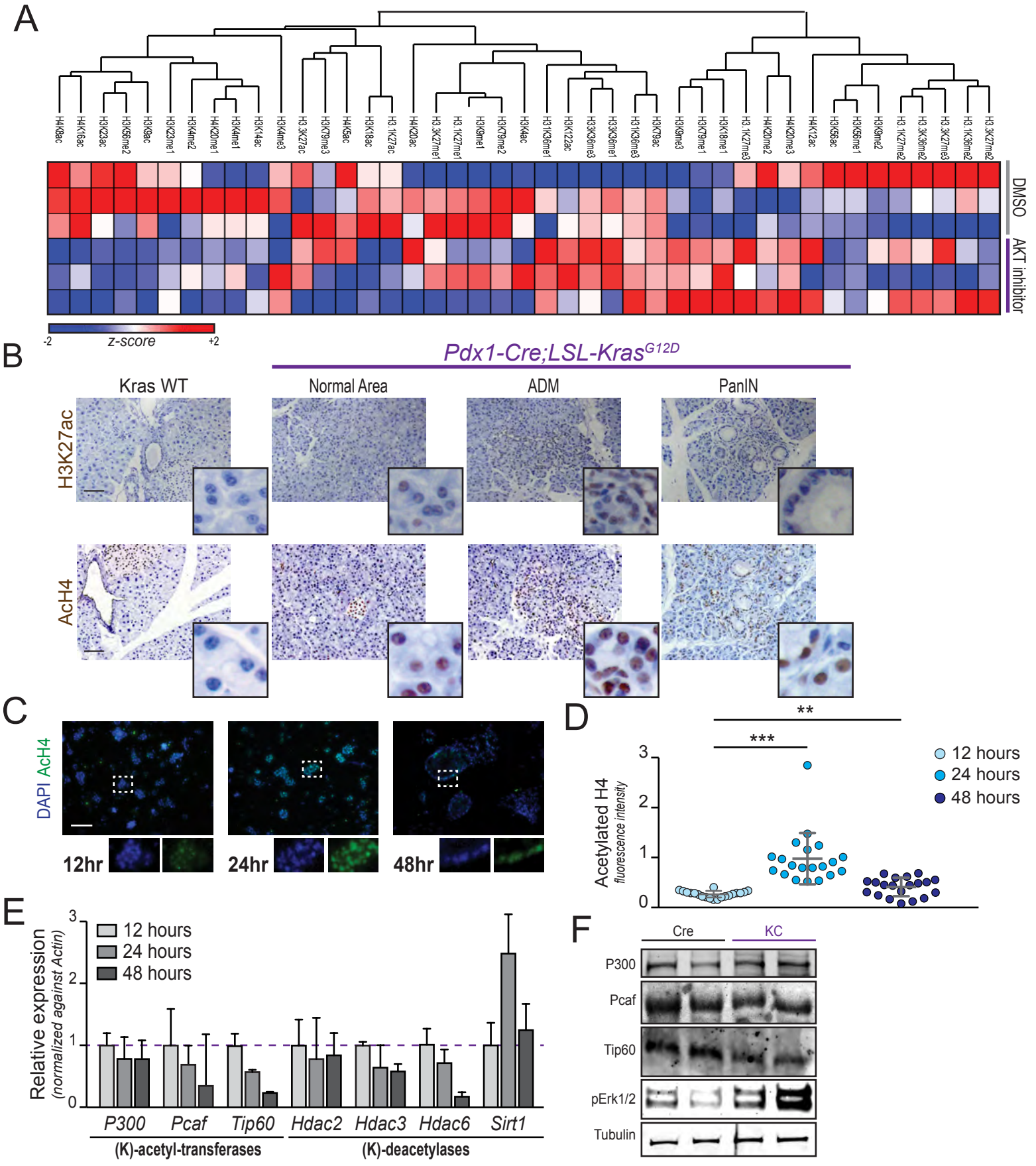

Histone acetylation is responsive to AKT inhibition and increases during acinar-to-ductal metaplasia (ADM). A, PanIN-derived pancreatic primary cells were treated with AKTi for 24 hours. Histone modifications were profiled by mass spectrometry. Heatmap shows regulation of detected histone marks. Rows show replicates (*n=3*, each treatment). **B,** Representative images of immunohistochemical staining against acetylated histones (H3K27ac, top panels; AcH4, bottom panels), nuclei counterstained with hematoxylin. Pancreata from either wild-type or $Kras^{G12D}$-expressing mice (*n=2*, each group) were harvested at different times (7 weeks of age, $Kras^{WT}$ and $Kras^{G12D}$ normal area; 4 months, $Kras^{G12D}$ ADM and PanIN) and fixed in formalin. Pictures show representative images from normal regions or areas containing the indicated lesions. Scale bar, 100 µm. **C,** Acinar cells were isolated from a 6-week-old KC mouse and embedded in Matrigel. At the indicated time, cell were fixed and subsequently stained for AcH4 (green) and counterstained with DAPI (blue). Bottom panels show individual channels. Scale bar,100 µm. Representative images from *n=2* biological replicates. **D,** quantification of C. Green fluorescence (AcH4) was quantified with ImageJ and normalized for relative blue fluorescence (DAPI). Each dot denotes an optical field (*n=25*, each time point). Error bars show mean +/- SD (**, p<0.01; ***, p<0.001). **E,** mRNA expression of KATs and KDACs in acinar cells at same time points as in panel C (*n=3*, each time point). Bars show mean +/- SD. **F,** Western blotting of acinar cells isolated from wild-type (Cre) or KC mice (*n=2*, each group). For all panels: scale bar, 100 µm.

Supplementary Figure S2

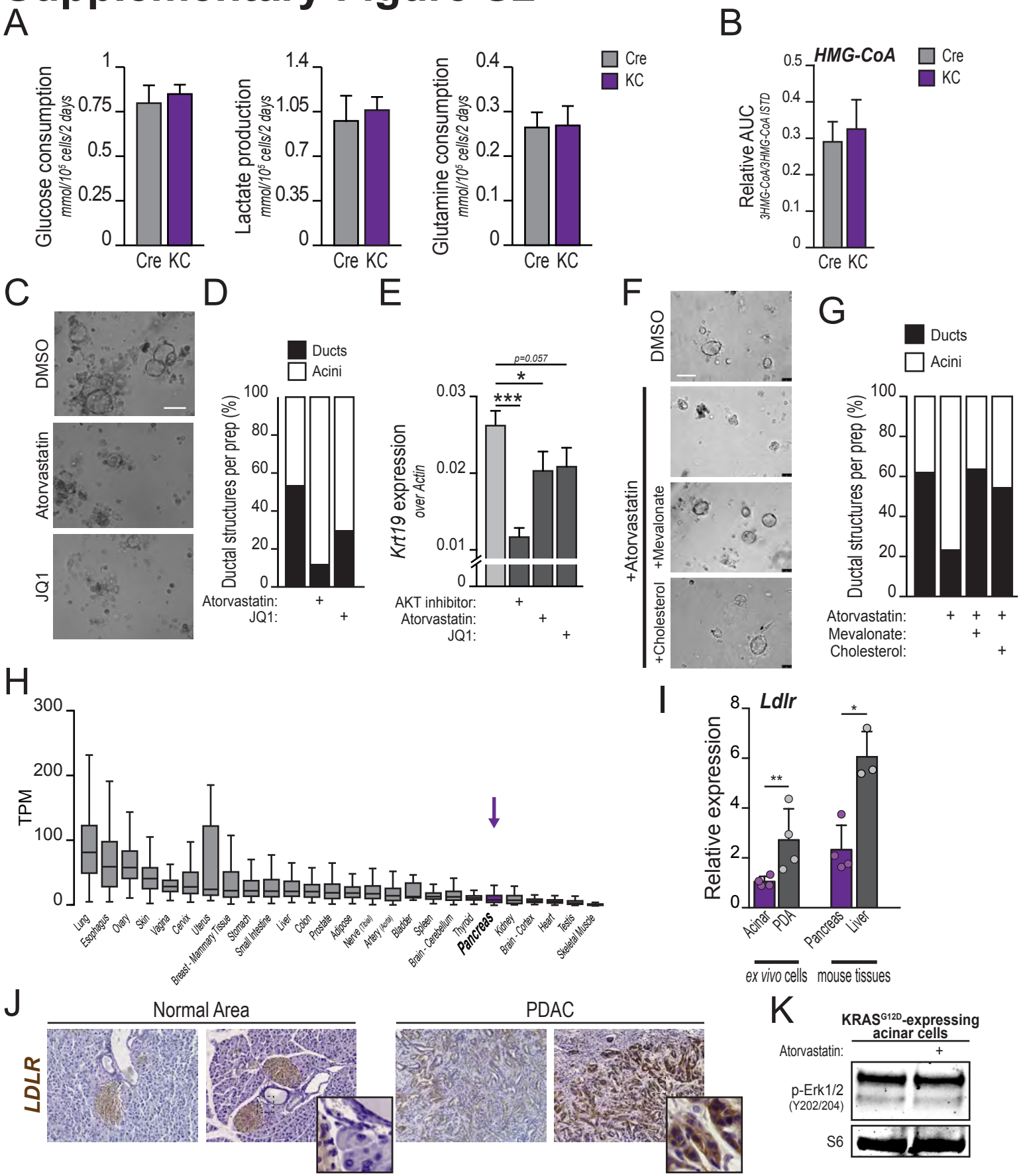

KRAS^{G12D} induces changes in acetyl-CoA metabolism. In panels A-G, pancreatic acinar cells were harvested from 6-8-week-old wild-type (*Pdx1-Cre*; **Cre**) or (*Pdx1-Cre;Kras^{G12D}*; **KC**) mice. Experimental replicates obtained from separate animals. **A,** Glucose and Glutamine consumption and lactate production in isolated acinar cells over 48 hours in culture (*n=3* mice, each group). **B,** LC-MS quantification of HMG-CoA in isolated acinar cells after 24 hours in culture (*n=4*, each group). **C,** morphology of matrigel-embedded KC acinar cells after 48 hours treatment with atorvastatin or JQ1 (n=3 mice, each group). Scale bar, 100 µm. **D,** quantification of (C), blinded. **E,** *Krt19* mRNA quantification of cells in Figure 2C. **F,** matrigel-embedded KC acinar cells after 48 hours treatment with atorvastatin, +/- mevalonate or cholesterol (n=3 mice, each group). Scale bar, 100 µm. **G,** quantification of (F), blinded. **H,** gene expression analysis of human heathy tissues, using publicly available datasets (GTex (29)). Tissues are listed according to mean level of expression and boxes show 75% CI, lines show median, minimum, maximum. Levels of expression in the pancreas are highlighted by a purple box. **I,** qPCR analysis of *Ldlr* gene expression (normalized over GAPDH), in isolated primary cells or whole mouse tissues. In purple, acinar cells or pancreata from WT animals. Dots denote individual animals. **J,** immunohistochemistry against LDLR, nuclei counterstained with hematoxylin. Pancreata from either wild-type (normal area) or Kras^{G12D}-expressing (PDAC) mice (n=3, each group) were used. Magnifications show poor expression in non-malignant acinar cells and elevated positivity in cancer epithelial cells. **K,** Western blotting of isolated acinar cells after 24 hours in culture, +/- atorvastatin (20µM). For all panels, error bars show mean, +/- SD (*, p<0.05; **, p<0.01; ***, p<0.001).

Supplementary Figure S3

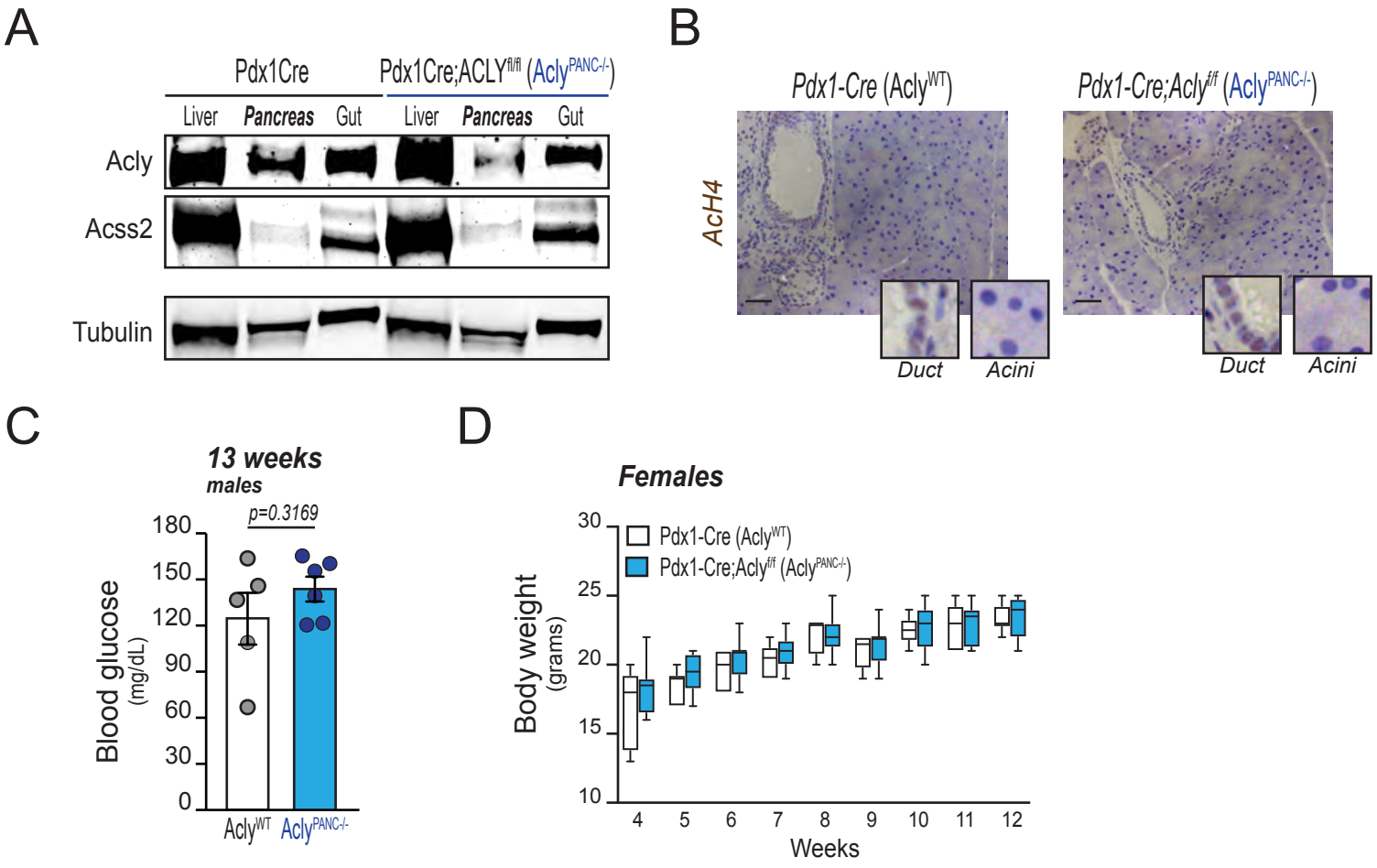

***Acly* deletion from murine pancreas does not cause overt metabolic abnormalities. A,** Western Blotting of whole organ lysates from 8-week-old mice. **B,** Immunohistochemistry against AcH4. Scale bars, 50 µm. **C,** blood glucose levels in overnight fasted animals. Each dot represents 1 mouse, mean +/- SEM. **D,** body weight over time in Acly^{WT} and Acly$^{PANC-/-}$ female mice (*n=5*, each group). Boxes show 75% CI, lines show median, minimum, maximum. Not statistically significant (repeated measures ANOVA with *Tukey-Kramer* adjustment for multiple comparisons).

Supplementary Figure S4

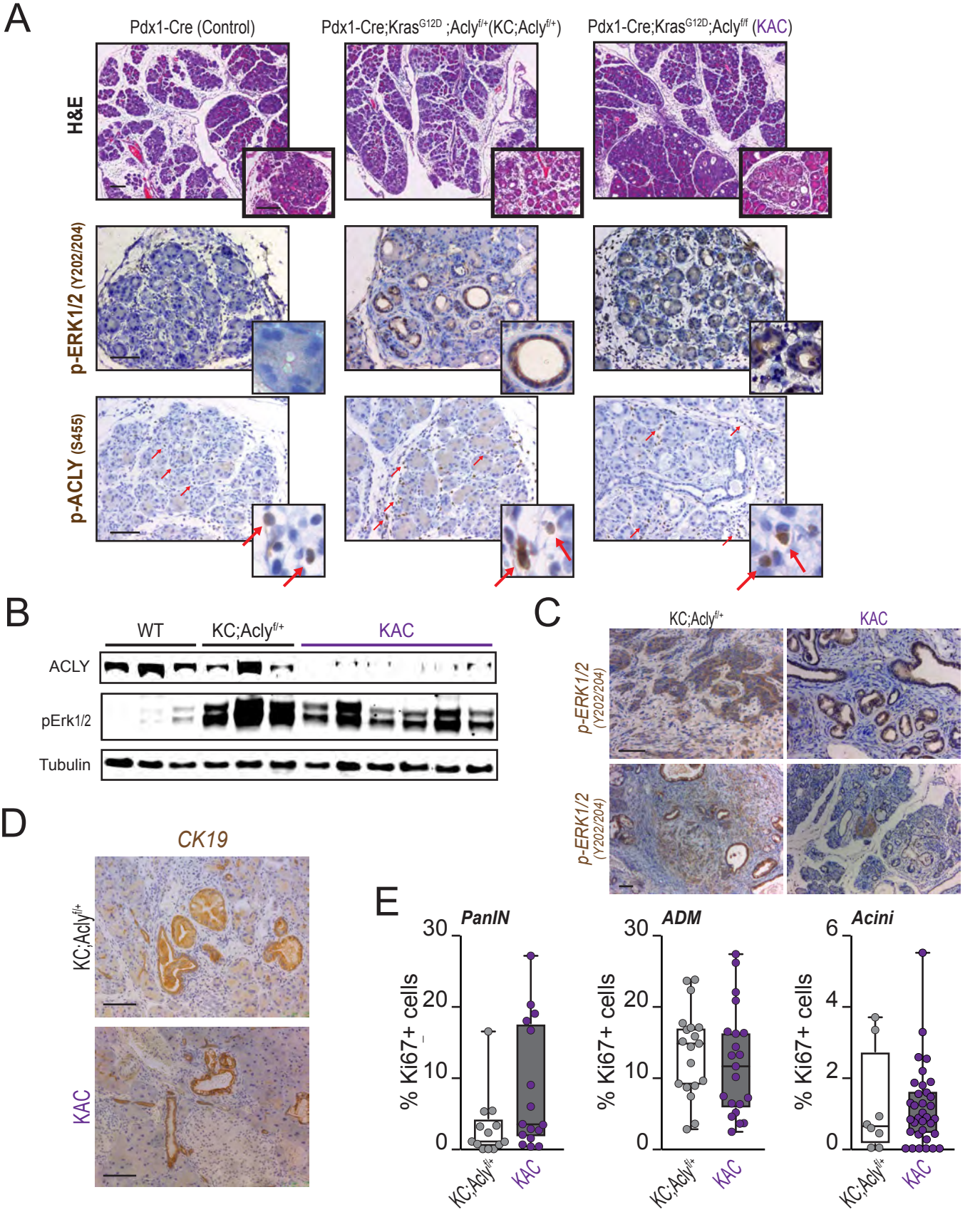

***Acly* deletion inhibits acinar-to-ductal metaplasia and impairs tumor formation. A,** Mice were treated with cerulein as illustrated in Figure 4F. Figure shows histological characterization of pancreata at *Day 3, acute phase*. Representative images for H&E staining and immunohistochemistry against p-ERK1/2(Y202/Y204) and p-ACLY(S455) are shown. Indents show magnifications. Red arrows indicate infiltrating cells (p-ACLY positive). **B,** Western Blotting of whole organ lysates from Day 21 Cre (WT), KC;Aclyf/+ or KAC mice. **C,** Immunohistochemistry against p-ERK1/2(Y202/Y204) in *Day 21* pancreata. Two magnifications. For immuhistochemistry, nuclei were counterstained with hematoxylin. **D,** Immunohistochemistry against Cytokeratin-19 (CK19) in *Day 21* pancreata. **E,** Immunohistochemistry against Ki67 (proliferation marker): quantifications. Ki67+ nuclei were counted in PanIN lesions, ADM foci, or normal acinar cells. 5 randomly selected optical fields per mouse section were evaluated. Optical fields with fewer than 75 acinar cells or 20 ADM cells or 20 PanIN cells were excluded from the analysis. Each dot represents an optical field. Boxes show 75% CI, lines show median, minimum, maximum. For all panels, scale bar, 100 µm.

Supplementary Figure S5

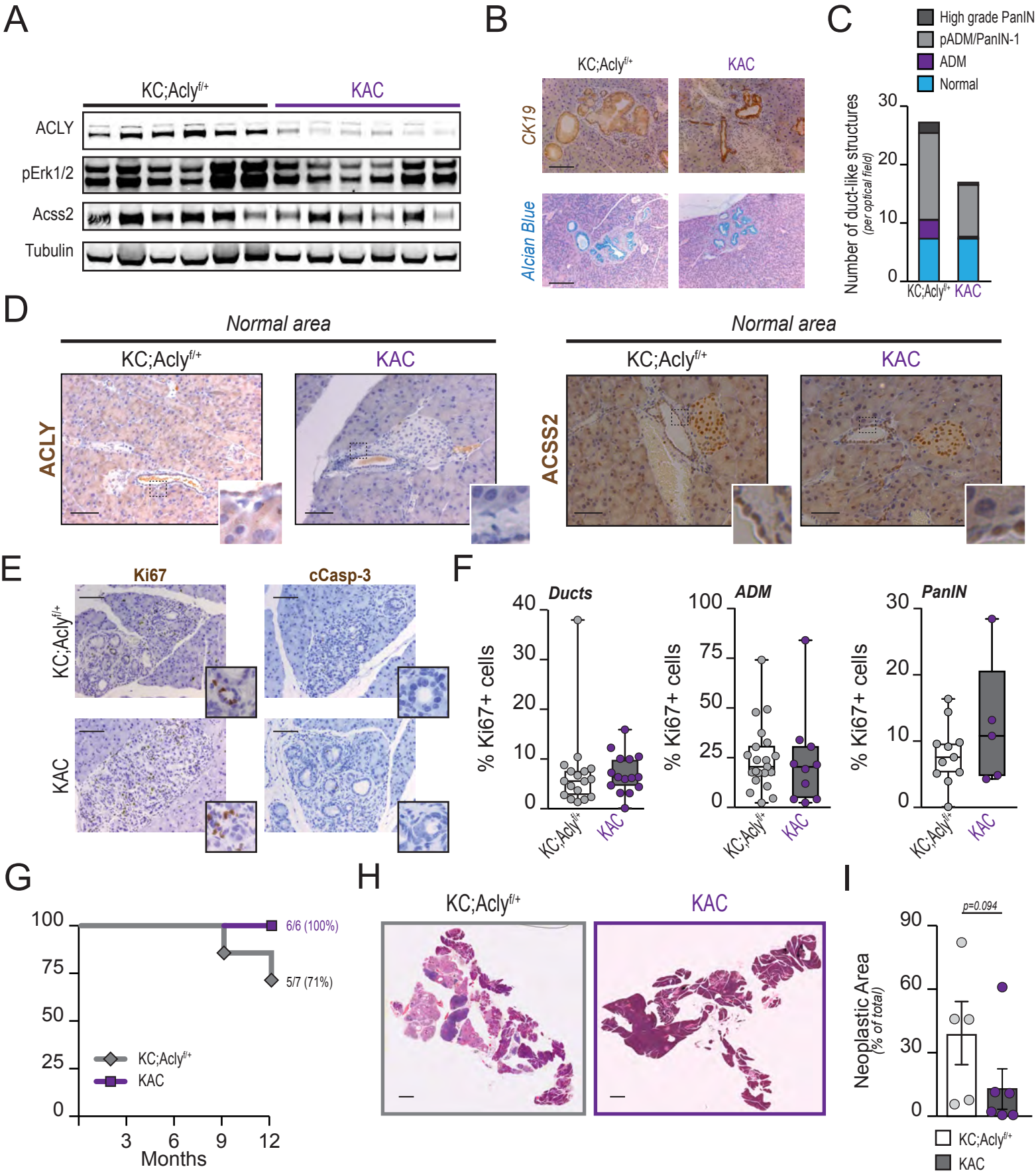

Pancreatic tumorigenesis is impaired in the absence of ACLY. Figure shows *Pdx1-Cre;Kras^{G12D};Acly$^{fl/+}$* (KC;Acly$^{fl/+}$) or *Pdx1-Cre;Kras^{G12D};Acly$^{fl/fl}$* (KAC). **A-F,** 4-month-old mice (*n*=7, each genotype). **G-I,** 1-year-old mice (*n*=5 KC;Acly$^{fl/+}$; *n*=6 KAC mice).
A, Western Blotting of whole pancreas lysates. **B,** staining of PanIN lesions using immunohistochemistry against CK19 (upper panels) or the acidic chemical dye Alcian Blue (bottom panels). Scale bar 100 μM. **C,** Lesions were blindly scored by a vet pathologist. 10 high-power optical fields per mouse section were analyzed Normal: normal, non-malignant duct; ADM: acinar-to-ductal metaplasia; pADM: polymorphic ADM; PanIN-1: pancreatic intra-epithelial neoplastic lesion type 1A or 1B; High grade PanIN: PanIN-2 or PanIN-3. **D,** immunohistochemistry against ACLY and ACSS2. Pictures show representative normal areas (not containing neoplastic ductal formations). Magnification shows duct and acinar cell nuclei. Scale bar, 50 μm. **E,** immuhistochemistry against Ki67 and cleaved Caspase-3 (cCasp-3). Nuclei counterstained with hematoxylin. Scale bar 100 μM. **F,** percent of Ki67+ nuclei in ducts, ADM foci and PanIN lesions. 5 randomly selected optical fields per mouse section were evaluated. Optical fields with fewer than 75 acinar cells or 20 ADM cells or 20 PanIN cells were excluded from the analysis. Each dot represents an optical field. Boxes show 75% CI, lines show median, minimum, maximum. **G,** Kaplan-Meier Survival to 1 year of age. **H,** hematoxylin and eosin (H&E) staining of 1-year-old KC;Acly$^{fl/+}$ or KAC mice, transverse section of whole pancreas. Scale bar, 1 mm. **I,** Each lesion's area and whole organ surface were measured in ImageJ. Lesions areas were summed and denoted as "neoplastic area". Percent of neoplastic area over total pancreas surface is shown. Each dot represents an animal. Bars show mean +/- SD.

Supplementary Figure S6

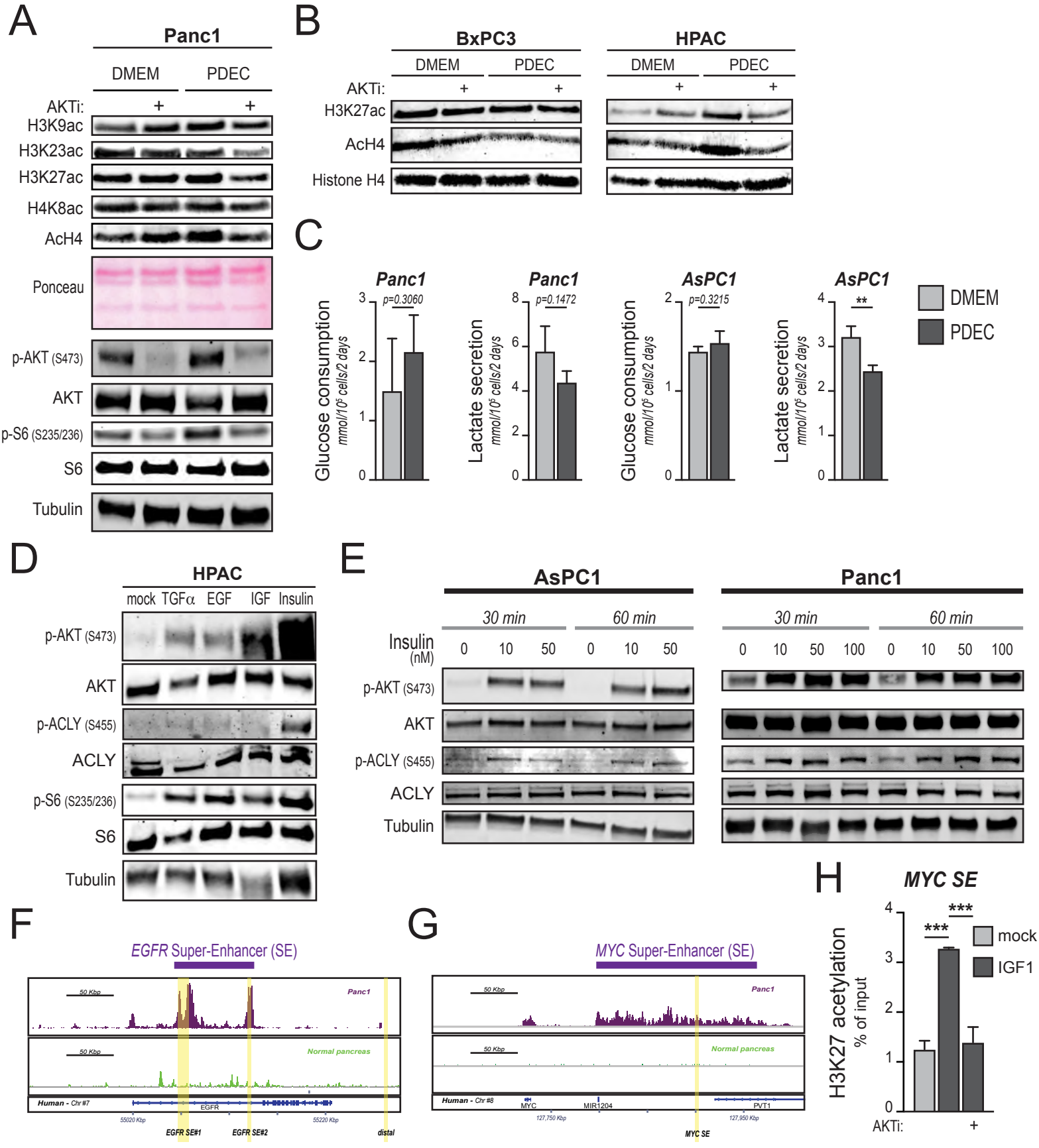

Environmental stimuli induce AKT-ACLY signaling and histone acetylation. A, Western blots of signaling and acid-extracted histones from Panc1 cells cultured in two different tissue culture media (DMEM or PDEC), +/- AKTi for 24 hours. Ponceau staining and tubulin are shown as loading controls for histones and signaling, respectively. **B,** BxPC3 and HPAC cells treated as in A. **C,** Glucose consumption, lactate production in indicated cell lines cultivated for 48 hours in either DMEM or PDEC medium. **D,** HPAC cells were serum-starved overnight, treated with indicated growth factors for 1 hour, and analyzed by western blot. **E,** AsPC1 and Panc1 cells reated with increasing doses of insulin for either 30 minutes or 1 hour. **F-G,** map of *EGFR* super-enhancer (F) or *MYC* super-enhancer (G) (labeled, purple dash). Tracks show H3K27ac profile of the *EGFR* and *MYC* loci, from publically-available ChIP-Seq data. Purple, Panc1 cells (ENCODE accession #: ENCBS729QZR). Green, normal human pancreas (ENCODE accession #: ENCSR612BWE). Structures and locations of the human genes present in the two loci are shown in blue. Locations of primer sets used are indicated. **H,** H3K27ac ChIP -QPCR of the *MYC* super-enhancer (SE). Bar graphs represent mean +/- SD, **, p<0.01; ***, p<0.0001.

Supplementary Figure S7

A

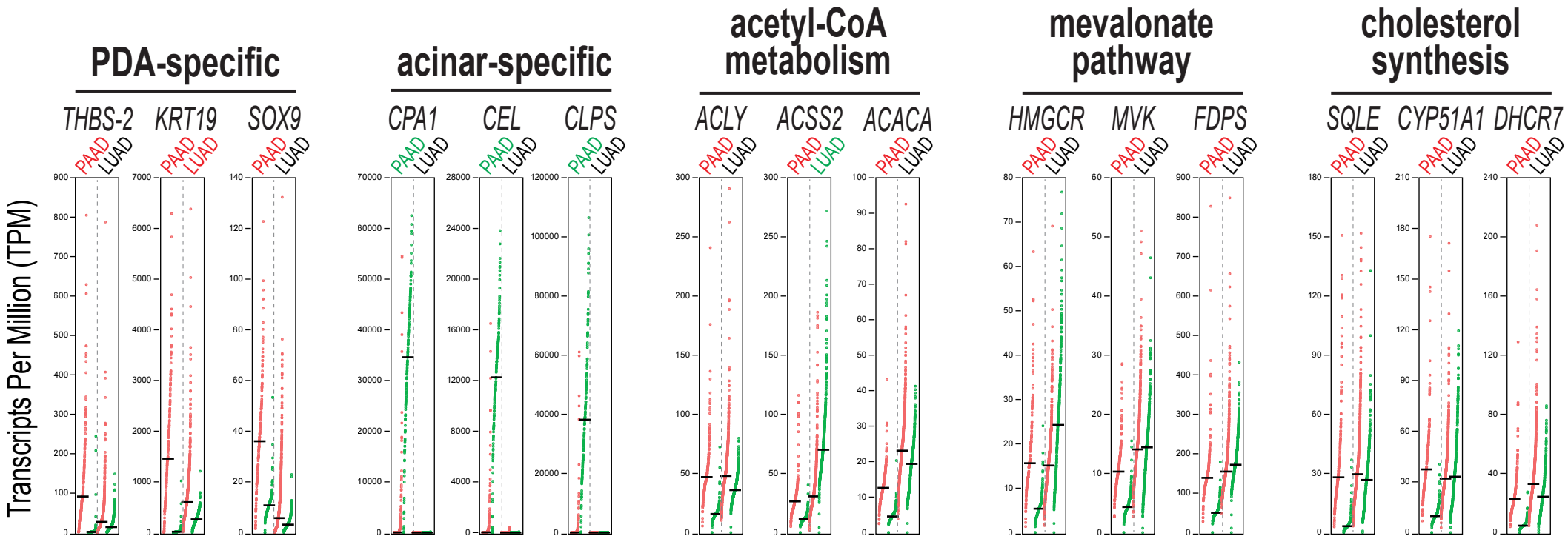

Normal tissues

Tumors

PAAD: Pancreatic ductal adeno carcinoma
LUAD: Lung adeno carcinoma
statistically upregulated
statistically downregulated
not significant

Genes encoding enzymes in acetyl-CoA metabolism and sterol synthesis are elevated in human PDA samples. A, gene expression analysis of human samples, using a public databases (GEPIA (36), see *Methods*). Expression in healthy tissues (green dots, data from GTEx consortium) or tumor tissues (red dots, data from TCGA consortium) was compared for PDA tumors (PAAD; compared to pancreatic tissues in GTEx) and lung adeno-carcinoma (LUAD; compared to healthy lung tissues in GTEx). Each dot represents a patient/donor (n=179 PDA tumors; n=171 normal pancreas; n=483 lung tumors; n=346 normal lung). Colors denote statistical significance: red marks upregulation in tumors, green marks downregulation (ANOVA; $p<0.05$).

Supplementary Table 1

Primers used in the manuscript

Primer Set	Sequence
Mouse Genotyping	
Cre-Fw	TGCCACGACCAAGTGACAGC
Cre-Rv	CCAGGTTACGGATATAGTTCATG
Acly_WT-Fw	TGCAATGCTGCCTCCAATGAT
Acly_WT-Rv	GGAGCCAGAGGAGAAAAAGGC
p53-Fw	AGCACATAGGAGGCAGAGAC
p53-Rv	CACAAAAACAGGTTAAACCCAG
tm1c (flox) -Fw	aaggcgcataacgataccac
tm1c (flox) -Rv	ccgcctactgcgactatagaga
Kras-WT	TGT CTT TCC CCA GCA CAG T
Kras-Common	CTG CAT AGT ACG CTA TAC CCT GT
Kras-mutant	GCA GGT CGA GGG ACC TAA TA
Gene expression (mouse)	
Hk2-Fw	TGA TCG CCT GCT TAT TCA CGG
Hk2-Rv	AAC CGC CTA GAA ATC TCC AGA
Hk1-Fw	GCACGA TGTTCTCTGGGGTG
Hk1-Rv	CGTCAAGA TGCTGCCAACCT
Pfk1-Fw	TGACATGACCATTGGCACAG
Pfk1-Rv	TCTTGCTACTCAGGATTCGG
Rpia-Fw	TGCAGCGAATAGCTGAAAGA
Rpia-Rv	ACAGCCATTCGAAGTTCCAC
Rpe-Fw	GGGGAATGGGATGAAGGTT
Rpe-Rv	GCACTGCCAGACACAATCAT
Dgat1-Fw	TGCTACGACGAGTTCTTGAG
Dgat1-Rv	CTCTGCCACAGCATTGAGAC
Slc7a5/Lat1-Fw	ATG GAG TGT GGC ATT GGC TT
Slc7a5/Lat1-Rv	TGC ATC AAC TTC TGG CAG AGC A
Bcat1-Fw	GATAATGGGTGTCAGCAGGTC
Bcat1-Rv	GGAGGAGTTGCCAGTTCTTCT
Pdha-Fw	GACTCAGGGTAGATGGAATGG
Pdha-Rv	CTTACGCTGGATGGGAACAC

Cs-Fw	GAACAGGTGTCTTGGCTCTC
Cs-Rv	CCTCATGGTCACTATGGATGG
Idh1-Fw	GCTGCTTCCAGTACTCTATCC
Idh2-Rv	GTGCAAACCTGATAAGGTCC
Ldha-Fw	CTCCAGCAAAGACTACTGTG
Ldha-Rv	TGGGTTAAGAGACTTCAGGG
Glut1-Fw	TGTGGTGTCGCTGTTTGTTGT
Glut1-Rv	CCTCGGGTGTCTTGTCACTT
Psat1-Fw	CAGTGGAGCGCCAGAATAGAA
Psat1-Rv	CCTGTGCCCCTTCAAGGAG
Gcnt3-Fw	CCTTTGGGCCACCCTCC
Gcnt3-Rv	CAAATTTTCGATGCAAGGGATC
P300-Fw	ggagcaagctaatggggaagtgag
P300-Rv	ccccagcatttttgagaggaagac
PCAF-Fw	CCGTGTCATTGGTGGTATCTGTT
PCAF-Rv	AGGAAGTTGAGGATCTCGTGCTT
mActin-Fw	TGGTGGGAATGGGTCAGAA
mActin-Rv	TCTCCATGTCGTCCCAGTTG
Gcn5-Fw	TGAGCAGGTCAAGGGTTATG
Gcn5-Rv	CGTAGGTGAGGAAGTAGAGAATG
Tip60-Fw	GTGAAACGGAAGGTGGAGGT
Tip60-Rv	CCAGTCATTCGTGGTGCTGA
mSirt1-Fw	GGGAACCTTTGCCTCATCTA
mSirt1-Rv	TACTGGAACCAACAGCCTTA
mHDAC1-Fw	TTGCTCGCTGCTGGACTTAC
mHDAC1-Rv	TGGCTTCTCCTCCTTGGTTT
mHDAC2-Fw	GGACAGGCTTGGTTGTTTCA
mHDAC2-Rv	ATTCCTACGACCTCCTTCAC
mHDAC3-Fw	CCGAAATGTTGCCCGGTGTT
mHDAC3-Rv	GGGTGCTTCTGGCCTGCTGT
mHDAC6-Fw	AACCGCACTGGGCTGGTCTA
mHDAC6-Rv	TCAAAGTTGGCACCTTCACG
18S-Fw	TCAACACGGGAAACCTCACC
18S-Rv	CCACCCACGGAATCGAGAAA
mKrt19-Fw	TCCCAGCTCAGCATGAAAGCT
mKrt19-Rv	AAAACCGCTGATCACGCTCTG
mACC1_Fw	ACAGTGGAGCTAGAATTGGAC
mACC1_Rv	ACTTCCCGACCAAGGACTTTG
mMvk_Fw	GCATCACCCTCCTGAAGC
mMvk_Rv	CTGGTCTCCCAGCAGTCAA
mFdps_Fw	GGAGGTCCTAGAGTACAATGCC
mFdps_Rv	AAGCCTGGAGCAGTTCTACAC
mHmgcs1_Fw	GGTCTGATCCCCTTTGGTG

mHmgcs1_Rv	TGTGAAGGACAGAGAACTGTGG
mHmgcr_Fw	CGTAAGCGCAGTTCCTTCC
mHmgcr_Rv	TTGTAGCCTCACAGTCCTTGG
mDgat1_Fw	TGCTACGACGAGTTCTTGAG
mDgat1_Rv	CTCTGCCACAGCATTGAGAC
mAcly-Fw	TTCGTCAAACAGCACTTCC
mAcly-Rv	ATTTGGCTTCTTGGAGGTG
mAcss2-Fw	GCTTCTTTCCCATTCTTCGGT
mAcss2-Rv	CCCGGACTCATTCAGGATTG
mFasn-Fw	ATTGGTGGTGTGGACATGGTC
mFasn-Rv	CCCAGCCTTCCATCTCCTG
mScd1-Fw	AGAGTCAGGAGGGCAGGTTT
mScd1-Rv	CTGGAGATCTCTTGGAGCATGT
mGAPDH-Fw	TCCTTTAGGATTTGGCCGT
mGAPDH-Rv	TTGATGGCAACAATCTCCAC
mG6pd-Fw	CCGGAAACTGGCTGTGCGCT
mG6pd-Rv	CCAGGTCACCCGATGCACCC
mGfpt1-Fw	ATGCAAGTGCCGTGATAG
mGfpt1-Rv	TCGTTTAATTCGGTGGATAGAG
mMgat5-Fw	CTGGACTGTGGATCTCAATAAC
mMgat5-Rv	ATGGCATATACGGCTCAATC
mCpa1-Fw	TCGATCACACACCGAGGGCT
mCpa1-Rv	GGGCATCCCAAAGGCAGCAT
mAmy2-Fw	CCTCATTGGGTTCTGCTGGGC
mAmy2-Rv	CGCCACTCGAACAGGTGGAC

Chromatin immuno precipitation (human)

EGFR#SE-065k-Fw	CAGAGCTGAAGGCAAGGGGA
EGFR#SE-065k-Rv	GGAGGCCTTCTCCAGGGTTC
EGFR#SE-075k-Fw	CCCAGACCATCAGTGGGCAG
EGFR#SE-075k-Rv	GGTGTGGAGGAAGCTGGAGG
EGFR#SE-131k-Fw	CTGGCTGCATCGTTCTGCTG
EGFR#SE-131k-Rv	CTCGCATGGTGCTGCTTCAG
EGFR#distal-217k-Fw	GAGGAGCCCTGAGTGGAAGC
EGFR#distal-217k-Rv	ACACCACTGTGTCAGCCACT
MYC#SE-Fw	TCCGGCAACACGTTCCCTTT
MYC#SE-Rv	AACACTCAACAGGCCAGCCC
LIF promoter-Fw	CCCTGCTGACCACTGTACCT
LIF promoter-Rv	TGAGTCAGTCACCCCTACCC
UPP1 promoter-Fw	TAGCTGCGACTCGAAGTGAA
UPP1 promoter-Rv	ACCTTCCTGATCCTGGGAGT

CXCL1 promoter-Fw	TATACAGCCCTGGCTTCCAC
CXCL1 promoter-Rv	CTGCTTGTTCCTTGTGTTGC
TUBA1A -Fw	CGA AAT GGC CTG GGT ATA TG
TUBA1A -Rv	CTG CAG AAG AAG CTC TGA AA